Proceedings of the 4th IFAC Conference on Analysis and Design of Hybrid Systems (ADHS 12) June 6-8, 2012. Eindhoven, The Netherlands

Observer design for DC/DC power converters with bilinear averaged model

Veaceslav Spinu * **Maarten Dam** ** **Mircea Lazar** *

* *Department of Electrical Engineering, Eindhoven University of Technology, P.O. Box 513, 5600 MB Eindhoven, The Netherlands. E-mails:* v.spinu@tue.nl, m.lazar@tue.nl.
** *TNO Technical Sciences / Automotive, P.O. Box 756, 5700AT Helmond, the Netherlands. E-mail:* maarten.dam@tno.nl.

Abstract: Increased demand for high bandwidth and high efficiency made full state-feedback control solutions very attractive to power-electronics community. However, full state measurement is economically prohibitive for a large range of applications. Moreover, state measurements in switching power converters are very noisy. These facts make the development of observer design targeted specifically to power electronics highly important. This paper analyses suitability of two previously proposed hybrid observer design techniques for continuous-time linear switched and discrete-time piecewise affine systems in context of power converters. Furthermore, a novel design procedure of Luenberger type observers is proposed for discrete-time systems with input-induced bilinearity. The performance of developed observers is demonstrated through simulation and experimental results obtained for a buck-boost converter.

Keywords: Observers, Power circuits, Switching functions, Piecewise linear analysis, Bilinear systems.

1. INTRODUCTION

Power converters are ubiquitous in consumer and industrial electronics. Both fields continuously demand higher efficiency, reliability and performance from converters. In this context advanced control techniques which rely on full state feedback rather than classic output feedback become increasingly attractive, see e.g., [Cortés et al., 2008, Mariéthoz et al., 2010, Spinu et al., 2011a,b]. However full state measurement may not be economically feasible in a wide range of applications. Moreover, measuring the inductor current is known to be a fairly complex task, as common mode voltage rejection is required, and it is very noisy due to ripple. As such, development of observer design techniques targeting power converters is of a paramount importance for the future development of the field.

Typical high efficiency power converter consists of, ideally lossless, linear storage elements interconnected by switches. Ideally, for a given state of switches the converter exhibits linear dynamics. There are two type of switches currently used in power converters, controlled, e.g., transistors, and elements with state dependent switching, e.g., diodes. As such a general, *continuous-time* (CT), model of a power converter is expressed as an affine switched differential equation with controlled and state-dependent switching.

In the context of digital control systems, *discrete-time* (DT) models are preferred and the computed control action is typically supplied to the modulator. Such models can be derived by using averaging techniques [Kazimierczuk, 2008]. By applying averaging a DT possibly nonlinear model of the system with continuous inputs is obtained. The typical non-linearity which appears in converter models is input-induced bilinearity. It appears when the energy is transferred from an internal storage element through a switch, e.g., from the inductor through transistor in a boost converter. Direct handling of nonlinear dynamics is not straightforward and, often, an approximated *piecewise affine* (PWA) model is used for the system.

Observer design for linear DT systems is a somewhat trivial problem, however the other three classes, i.e., CT switched affine, DT bilinear and PWA plant models raise considerable difficulties.

In this paper the attention is concentrated on the synthesis of Luenberger type observers for CT switched affine, DT systems with PWA dynamics, and input-induced bilinearity. First two observer design techniques are based on previous works, [Alessandri and Coletta, 2001b] and [Heemels et al., 2008], respectively, and a novel hybrid observer synthesis method is proposed for the DT-B model.

All three synthesis techniques are compared through simulations. Experimental results of DT observers on a buck-boost converter setup are also provided.

2. PRELIMINARIES

This section explains some mathematical notations and definitions used in this paper.

Let $\mathbb{R}$, $\mathbb{R}_+$, $\mathbb{Z}$ and $\mathbb{Z}_+$ denote the set of real numbers, the set of non-negative reals, the set of integer numbers and non-negative integers, respectively. $\mathbb{R}^{n\times m}$ denotes the set of real $n \times m$ matrices. For a matrix $Z \in \mathbb{R}^{n\times m}$, $[Z]_{ij} \in \mathbb{R}$ denotes the element on the i-th row and the j-th column of Z, $[Z]_{i\bullet} \in \mathbb{R}^{1\times m}$ denotes the i-th row of Z and $[Z]_{\bullet j} \in \mathbb{R}^{n\times 1}$ denotes the j-th column of Z. $\mathbf{1}_p \in \mathbb{R}^p$ is a vector with $[\mathbf{1}_p]_i = 1$ for all $i \in \mathbb{Z}_{[1,p]}$, $p \in \mathbb{Z}_{\geq 1}$ Given a vector $x \in \mathbb{R}^n$, $\|x\|_p$ denotes the p-norm of x, $\|x\|$ denotes an arbitrary norm of x.

Given two sets $\mathbb{P}, \mathbb{S} \in \mathbb{R}^n$, $\mathbb{P}_{\mathbb{S}} := \mathbb{P} \cap \mathbb{S}$, and $\mathrm{Co}(\mathbb{P})$ denote the convex hull of all points in $\mathbb{P}$.

The next lemma is an application of the Schur complement [Boyd et al., 1994].

Lemma 2.1. When $Q = Q^\top$ and $R = R^\top$ the following matrix inequalities are equivalent

$$\begin{bmatrix} Q & S \\ S^\top & R \end{bmatrix} \succ 0, \tag{1}$$

$$\begin{aligned} R &\succ 0, \\ Q - SR^{-1}S^\top &\succ 0. \end{aligned} \tag{2}$$

In matrices $*$ denotes the transposed, e.g.,

$$\begin{bmatrix} A & B \\ * & C \end{bmatrix} \Longleftrightarrow \begin{bmatrix} A & B \\ B^\top & C \end{bmatrix}.$$

Definition 2.2. A polyhedron (or a polyhedral set) in $\mathbb{R}^n$ is a set obtained as the intersection of a finite number of open and/or closed half-spaces. A polyhedron $\mathbb{P} \subset \mathbb{R}^n$ has an $\mathcal{H}$-representation:

$$\mathbb{P} := \{x \in \mathbb{R}^n | P_e x \leq \mathbf{1}_{p_e},\ P_i x < \mathbf{1}_{p_i}\}$$

where $P_e \in \mathbb{R}^{p_e \times n}$,$P_i \in \mathbb{R}^{p_i \times n}$ and $p_e,\ p_i \in \mathbb{Z}_{\geq 1}$.

Let $\mathcal{P}(\mathbb{R}^n)$ denote the set of all bounded and non-empty polyhedrons in $\mathbb{R}^n$. Given a polyhedron $\mathbb{P} \in \mathcal{P}(\mathbb{R}^n)$, the map $\mathrm{vert} : \mathcal{P}(\mathbb{R}^n) \rightrightarrows \mathbb{R}^n$ provides the set of vertices of $\mathrm{cl}(\mathbb{P})$.

Consider the following two autonomous systems

$$x^+ = \phi_d(x), \tag{3}$$

$$\dot{x} = \phi_c(x), \tag{4}$$

with $\phi_c(0) = \phi_d(0) = 0$.

A function $\alpha : \mathbb{R}_+ \to \mathbb{R}_+$ belongs to class $\mathcal{K}_\infty$ if it is continuous, strictly increasing, $\alpha(0) = 0$ and $\lim_{s\to\infty} \alpha(s) = \infty$.

Theorem 2.3. Let $\alpha_1, \alpha_2 \in \mathcal{K}_\infty$, $\rho \in \mathbb{R}_{(0,1)}$ and let $V : \mathbb{R}^n \to \mathbb{R}$ be a function such that:

$$\alpha_1(\|x\|) \leq V(x) \leq \alpha_2(\|x\|),\ \forall x \in \mathbb{R}^n, \tag{5a}$$

$$V(\phi_d(x)) \leq \rho V(x),\ \forall x \in \mathbb{R}^n. \tag{5b}$$

Then system (3) *is asymptotically stable in $\mathbb{R}^n$.*

Definition 2.4. The function V that satisfies (5) is called a *Lyapunov function in* $\mathbb{R}^n$ and ρ is called the contraction rate of V.

The counterpart of Theorem 2.3 for the continuous time autonomous system (4) follows.

Theorem 2.5. Let $V : \mathbb{R}^n \to \mathbb{R}$ be a function such that $V(0) = 0$ and $V(x) > 0$ for all $x \in \mathbb{R}^n_{\neq 0}$. Furthermore, let

$$\dot{V}(\phi_c(x)) \leq -\rho V(x),\ \forall x \in \mathbb{R}^n, \tag{6}$$

for some $\rho \in \mathbb{R}_{>0}$. Then system (4) *is asymptotically stable in $\mathbb{R}^n$.*

3. SYSTEM DESCRIPTION

Prior to observer synthesis the system model has to be defined. Fast switching dynamics of power converters makes analysis of the system properties challenging. As such, several modelling strategies were developed in the field. Three most common approaches to power converter modelling are summarized in following subsections. To support modelling procedures, schematic representation of two classic converter topologies are shown in Figure 1, i.e., buck and boost converters.

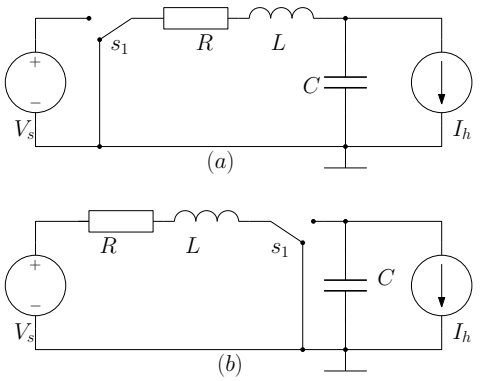

Fig. 1. Schematics of the buck *(a)* and the boost *(b)* DC/DC power converters.

3.1 Continuous-time switched affine model

As mentioned before, high efficiency DC/DC power converters generally comprise of linear components, e.g., capacitors and inductors, which are interconnected by switching elements. As such, general continuous-time model of the converter is

$$\begin{aligned} \dot{x} &= A(s)x + B(s)w + f, \\ y &= Cx, \end{aligned} \tag{7}$$

where $x \in \mathbb{R}^n$ is the system state, i.e., capacitor voltages and inductor currents, $[s]_i \in \mathbb{Z}_{[0,l_i]}$,$i = \mathbb{Z}_{[1,m]}$ denote the state of the switch i, $w \in \mathbb{R}^v$ are the exogenous signals applied to the converter, e.g., input voltage and output current, $y \in \mathbb{R}^o$ denote available state measurements. Vector f contains additive constant terms such as forward voltage of a switch. Matrices $A(s)$ and $B(s)$ have the following form

$$A(s) := \begin{bmatrix} s^\top \mathcal{A}_1 \\ \vdots \\ s^\top \mathcal{A}_n \end{bmatrix} + \mathcal{A}_0,\ B(s) := \begin{bmatrix} s^\top \mathcal{B}_1 \\ \vdots \\ s^\top \mathcal{B}_n \end{bmatrix} + \mathcal{B}_0, \tag{8}$$

where $\mathcal{A}_0 \in \mathbb{R}^{n\times n}$, $\mathcal{B}_0 \in \mathbb{R}^{n\times v}$, $\mathcal{A}_i \in \mathbb{R}^{m\times n}$ and $\mathcal{B}_i \in \mathbb{R}^{m\times v}$ for $i \in \mathbb{Z}_{[1,n]}$.

Remark 3.1. Note that a typical switching element has two positions, e.g., open or closed, when the switching element has multiple positions it can be modelled as multiple two position switches. As such, the CT-SA model of a power converter (7) which has $l_i = 1$ for all $i \in \mathbb{Z}_{[1,m]}$ generally can be derived. Without loss of generality $l_i = 1$ assumed throughout the paper. □

The vector s can assume only a limited number of values, i.e., 2^m according to the Remark 3.1. Let $\mathbb{S} := \{s_j\}_{j\in\mathbb{Z}_{[1,2^m]}}$ be the set of all possible states of switches, and for each s_j, $A_j := A(s_j)$ and $B_j := B(s_j)$. With this notation (7) becomes a *continuous-time switched affine* (CT-SA) model

$$\begin{aligned} \dot{x} &= A_j x + B_j w + f, \quad \text{if} \quad s = s_j, \\ y &= Cx, \end{aligned} \tag{9}$$

where $A_j := A(s_j)$ and $B_j = B(s_j)$.

3.2 Averaged discrete time bilinear model

When the converter is controlled by a fixed frequency *pulse-width modulated* (PWM) signal a very useful modelling technique is averaging. In this way, the function of a switch becomes equivalent to a transformer but applicable to DC signals. The continuous time averaged model of the power converter

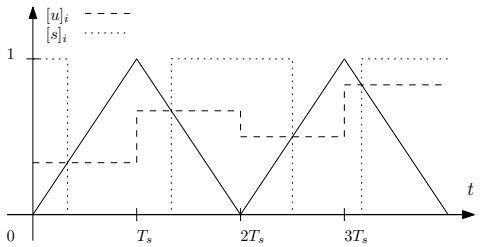

Fig. 2. Example of a PWM waveform generated by the control signal $[u]_i \in \mathbb{R}_{[0,1]}$ with T_s half of the PWM cycle. $[u]_i$ is marked with dashed line, switch state $[s]_i$ with dotted line and the internal triangular signal of the modulator with solid line.

is of the same form as (7) with the only difference that the switch state s is changed to $u \in \mathbb{R}^m_{[0,1]}$, which is the vector of duty-cycle ratios for each switching element. The averaging is performed for a time interval T_s, which is typically a multiple of half PWM periods and is equal to the sampling time of the controller. As such, this model describes converter behaviour only at the sampling instants and is discretized in practice. A typical PWM waveform is shown in Figure 2.

The model (7) has input-induced bilinearity, i.e., it contains products $[u]_i[x]_j$ and $[u]_i[w]_j$. Thus, the discretization is typically done by Euler forward method. After discretization, one obtains *discrete-time averaged bilinear* (DT-B) model of the power converter

$$\begin{aligned} x^+ &= (I_n + T_s A(u))x + T_s B(u)w + T_s f, \\ y &= Cx. \end{aligned} \tag{10}$$

As the switching period of the converter is very small comparing to time constants of output filters, the DT-B model captures well the converter dynamics regardless to approximation errors introduced by the discretization method.

3.3 Approximation with discrete time PWA model

Dealing with nonlinear models is generally difficult. As such, a *discrete-time piecewise affine* (DT-PWA) approximation of the DT-B converter model is often employed for controller and observer synthesis. The DT-PWA approximation of the DT-B model can be computed as follows.

Let the domain of variation of x, u and w, i.e.,

$$\mathcal{D} = \{ \begin{bmatrix} x \\ u \\ w \end{bmatrix} | x \in \mathbb{X} \in \mathcal{P}(\mathbb{R}^n),\ u \in \mathbb{R}^m_{[0,1]},\ w \in \mathbb{W} \in \mathcal{P}(\mathbb{R}^v) \},$$

be partitioned into polyhedral regions $\{\mathbb{P}_j\}_{j \in \mathbb{Z}_{[1,s]}}$, such that, $\bigcup_{j \in \mathbb{Z}_{[1,s]}} \mathbb{P}_j = \mathcal{D}$ and $\mathbb{P}_i \cap \mathbb{P}_j = \emptyset$ for all $i, j \in \mathbb{Z}_{[1,s]}$, $i \neq j$.

Then for each $j \in \mathbb{Z}_{[1,s]}$, a finite set of points of interest $\mathcal{S}_j \subset \mathbb{P}_j$ is selected. Next an optimizations problem is solved such that the error in between the affine model corresponding to $\mathbb{P}_j$ and the value of the DT-B model is minimized over $\mathcal{S}_j$. As a solution to this optimization problem, one recovers the DT-PWA approximation of the DT-B converter model,

$$x^+ = \bar{A}_i x + \bar{B}_i u + \bar{W}_i w + \bar{f}_i, \text{ if } \begin{bmatrix} x \\ u \\ w \end{bmatrix} \in \mathbb{P}_i. \tag{11}$$

The DT-PWA model demands slightly more computation power in the real-time, i.e., the vector $\begin{bmatrix} x \\ u \\ w \end{bmatrix}$ has to be located within $\{\mathbb{P}_i\}_{i \in \mathbb{Z}_{[1,s]}}$. Nevertheless, it makes a range of controller and observer synthesis techniques applicable.

4. OBSERVER SYNTHESIS

This section provides a Luenberger type observer synthesis technique for each model given in Section 3. Observer synthesis methods for CT-SA and DT-PWA models have some similarities and will be presented first. Then, a novel hybrid observer design method is proposed which is applicable to systems with DT-B model.

Prior to the observer synthesis several assumptions are made.

Assumption 4.1. At each time instant the state of switches s is known.

Typically observers are computed on the same platform with controllers, thus a communication between them ensures that the state of all controlled switches is known. Precise commutation of uncontrolled switches can be forced by maintaining the converter in continuous conduction mode.

Assumption 4.2. The region of DT-PWA model, $\mathbb{P}_i \subseteq \bar{\mathbb{P}}$, such that $\begin{bmatrix} x \\ u \\ w \end{bmatrix} \in \mathbb{P}_i$, is known at each moment of time.

As the u introduces the bilinearity into the DT-B model, it is reasonable to partition $\bar{\mathbb{P}}$ with respect to u only. This strategy coupled with Assumption 4.1 satisfies the statement of Assumption 4.2.

Assumption 4.3. External signals w are measurable.

4.1 Observer synthesis for CT-SA model

Let begin with writing the state estimation equation for the CT-SA model (9) when $s = s_i$,

$$\begin{aligned} \dot{\hat{x}} &= A_i \hat{x} + B_i w + f + L_i(y - \hat{y}), \\ \hat{y} &= C\hat{x}, \end{aligned}$$

where $L_i \in \mathbb{R}^{n \times o}$ is the observer gain and $i \in \mathbb{Z}_{[1,2^m]}$. Under the Assumption 4.1, the error dynamics $e := x - \hat{x}$ can be written as,

$$\dot{e} = (A_i - L_i C)e. \tag{12}$$

Theorem 4.4. Let,

$$(A_i - L_i C)^\top P + P(A_i - L_i C) \prec -\rho P, \tag{13}$$

be satisfied for all $i \in \mathbb{Z}_{[1,2^m]}$, some symmetric positive definite matrix $P \in \mathbb{R}^{n \times n}$ and some $\rho \in \mathbb{R}_{>0}$. Then the error dynamics (12) *is globally asymptotically stable.*

For the proof of this theorem refer to Theorem 2.2 in [Alessandri and Coletta, 2001b]. To solve the inequality (13) of Theorem 4.4 the following Lemma is introduced.

Lemma 4.5. Let

$$(PA_i - Y_i C)^\top + (PA_i - Y_i C) \prec -\rho P, \tag{14}$$

be satisfied for some symmetric positive definite matrix P, some Y_i, $i \in \mathbb{Z}_{[1,2^m]}$ and $\rho \in \mathbb{R}_{>0}$. Then the inequality (13) *is satisfied with P and by taking $L_i = P^{-1}Y_i$.*

The proof of the Lemma 4.5 is discussed in Problem 2.4 in [Alessandri and Coletta, 2001b]. Note that the LMI (14) can be solved for a single $Y = Y_i$, for all $i \in \mathbb{Z}_{[1,2^m]}$, and yields a common observer gain for all modes of the converter $L = L_i$.

4.2 Observer synthesis for DT-PWA model

The observer design technique for the DT-PWA model is very similar to the CT-SA. When $\begin{bmatrix} \hat{x} \\ u \\ w \end{bmatrix} \in \mathbb{P}_i$ the Luenberger observer

can be written as follows,

$$\begin{aligned}\hat{x}^+ &= \bar{A}_i\hat{x} + \bar{B}_i u + \bar{W}_i w + \bar{f}_i + L_i(y - \hat{y}) \qquad (15)\\ \hat{y} &= C\hat{x}.\end{aligned}$$

From Assumption 4.2 it follows that for any $\left[\begin{smallmatrix}\hat{x}\\ u\\ w\end{smallmatrix}\right] \in \mathbb{P}_i$, $\left[\begin{smallmatrix}x\\ u\\ w\end{smallmatrix}\right] \in \mathbb{P}_i$, and as such, the error dynamics is

$$e^+ = (\bar{A}_i - L_i C)e. \qquad (16)$$

Theorem 4.6. Suppose there exist a positive definite matrix P and a number $\rho \in \mathbb{R}_{(0,1)}$ and

$$(\bar{A}_j - L_j C)^\top P(\bar{A}_j - L_j C) \preceq \rho P, \qquad (17)$$

hold for all $j \in \mathbb{Z}_{[1,s]}$. Then the error dynamics (16) *is globally asymptotically stable.*

To solve the inequality (17) in Theorem 4.6 the following lemma is introduced.

Lemma 4.7. Suppose that

$$\begin{bmatrix} \rho P & \bar{A}_j^\top P - C^\top Y_j \\ P\bar{A}_j - Y_j^\top C & P \end{bmatrix} \succeq 0. \qquad (18)$$

hold for all $j \in \mathbb{Z}_{[1,s]}$, and some $P \succ 0$, $\rho \in \mathbb{R}_{(0,1)}$ and Y_j. Then the inequality (17) *holds with P, ρ and $L_j = (Y_j P^{-1})^\top$, respectively.*

For the proof of Theorem 4.6 and Lemma 4.7, interested reader is referred to Theorem 1 and Lemma 1 from [Alessandri and Coletta, 2001a], respectively. As in case of the CT-SA observer, it is possible to compute a single gain $L = L_i$ for the DT-PWA observer by considering a single $Y = Y_i$ in (18).

Remark 4.8. A better approximation of the DT-B model, comparing to the DT-PWA, can be obtained with the piecewise model of the following form

$$x^+ = \bar{A}_i x + \bar{B}_i u + B(u)w + \bar{f}_i, \text{ if } \begin{bmatrix}x\\ u\\ w\end{bmatrix} \in \mathbb{P}_i. \qquad (19)$$

Under Assumption 4.1 and Assumption 4.2, the error dynamics remains unchanged. As such the observer synthesis method described in this section is applicable to system (19) also.

Remark 4.9. Although, in this paper it is assumed that converter mode, i.e., $s = s_i$ is known, the observer design can be extended to handle the situations when Assumption 4.1 does not hold, e.g., discontinuous conduction mode in power converters. See [Juloski et al., 2003] for more details for the case when system mode has to be estimated as well.

4.3 Observer synthesis for DT-B model

Let $\mathcal{U} := \{\mathbb{U}_i\}_{i\in\mathbb{Z}_{[1,h]}}$, where $\mathbb{U}_i$ is a bounded and non-empty polyhedron, such that, $\mathbb{U}_i \cap \mathbb{U}_j = \emptyset$ for all $i, j \in \mathbb{Z}_{[1,h]}$, $i \neq j$, and $\cup_{i\in\mathbb{Z}_{[1,h]}}\mathbb{U}_i = \mathbb{R}^m_{[0,1]}$. A separate observer gain will be synthesized for each polyhedral set $\mathbb{U}_i$, $i \in \mathbb{Z}_{[1,h]}$.

As for the other two observers, one recovers the following state estimation equation and error dynamics for the DT-B model,

$$\hat{x}^+ = A(u)\hat{x} + B(u)w + f + L_i(y - C\hat{x}), \qquad (20)$$

$$e^+ = (A(u) - L_i C)e, \qquad (21)$$

when $u \in \mathbb{U}_i$.

Theorem 4.10. Suppose that there is a symmetric positive definite matrix P, a number $\rho \in \mathbb{R}_{(0,1)}$ and the observer gains $L_i = (Y_i P^{-1})^\top$, such that,

$$\begin{bmatrix} \rho P & (PA(v_j) - Y_i^\top C)^\top \\ * & P \end{bmatrix} \succeq 0,\ \forall v_j \in \mathrm{vert}(\mathbb{U}_i), \qquad (22)$$

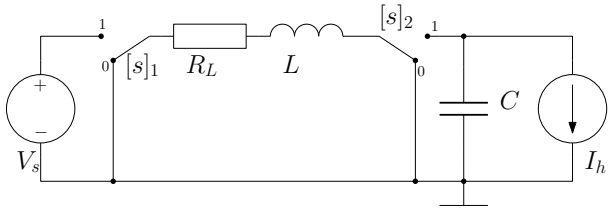

Fig. 3. Schematic representation of a buck-boost converter.

holds for all $i \in \mathbb{Z}_{[1,h]}$. Then the error dynamics (21) *is exponentially stable.*

Proof. Let $u \in \mathbb{U}_i = \mathrm{Co}(\mathrm{vert}(\mathbb{U}_i))$.
Thus $u = \sum_{v_j\in\mathrm{vert}(\mathbb{U}_i)} \lambda_j v_j$, for some λ_j such that $\sum_{j=1}^{|\mathrm{vert}(\mathbb{U}_i)|} \lambda_j = 1$. As such,

$$P\begin{bmatrix} u^\top\mathcal{A}_1 \\ \vdots \\ u^\top\mathcal{A}_n \end{bmatrix} = \sum_{v_j\in\mathrm{vert}(\mathbb{U}_i)} \left(\lambda_j P \begin{bmatrix} v_j^\top\mathcal{A}_1 \\ \vdots \\ u^\top\mathcal{A}_n \end{bmatrix}\right). \qquad (23)$$

By employing (23) one can show that

$$\begin{bmatrix} \rho P & (PA(u) - Y_i^\top C)^\top \\ * & P \end{bmatrix} = \sum_{v_j\in\mathrm{vert}(\mathbb{U}_i)} \left(\lambda_j \begin{bmatrix} \rho P & (PA(v_j) - Y_i^\top C)^\top \\ * & P \end{bmatrix}\right) \succeq 0, \qquad (24)$$

for all $u \in \mathbb{U}_i$. By employing Lemma 2.1 one recovers,

$$\rho P - (PA(v_j) - Y_i^\top C)^\top P^{-1}(PA(v_j) - Y_i^\top C) \succeq 0,$$

which is equivalent to

$$\rho P - (A(v_j) - L_i C)^\top P P^{-1} P(A(v_j) - L_i C) \succeq 0. \qquad (25)$$

As (24) is valid for all $i \in \mathbb{Z}_{[1,l]}$, (25) implies that

$$\rho e^\top P e - (e^+)^\top P e^+ \geq 0. \qquad (26)$$

Consider the following function $V(e) := e^\top P e$. Equation (26) shows that $V(e)$ is the Lyapunov function for the error dynamics. Thus the error dynamics is globally asymptotically stable. □

Remark 4.11. It is possible to obtain a single gain L when $\mathbb{U}_1 = \mathbb{R}^m_{[0,1]}$. However, it can be done also by enforcing continuity at the boundary of two adjacent regions by,

$$PA(v_j) - Y_i^\top C = PA(v_j) - Y_j^\top C,\ v_j \in \mathbb{U}_i \cap \mathbb{U}_j,\ i \neq j.$$

The results of these two methods can differ, as the second method slightly reduces the conservatism and may return a feasible solution for smaller values of ρ. □

5. SIMULATION AND EXPERIMENTAL RESULTS

The three approaches to state observer synthesis given in Section 4 are applied to state-estimation for a buck-boost DC/DC converter. The schematic of a buck-boost converter is given in Figure 3. System state vector is defined as $x := \left[\begin{smallmatrix} v_C \\ i_L \end{smallmatrix}\right]$, where v_C is voltage across capacitor and i_L is the current through the inductor. The external signals $w := \left[\begin{smallmatrix} V_s \\ I_h \end{smallmatrix}\right]$ are the supply voltage V_s and the output current I_h.

Typically, measuring v_C does not impose any difficulty in real-life applications. On the other hand, measuring the i_L is a rather difficult task. Thus, in this example the capacitor voltage is considered to be measured and the inductor current is estimated.

Table 1. Component values for the buck-boost power converter

Name	Value
V_s	10 V
I_h	0.2 A
C	22μF
L	220μH
R_L	0.2Ω

Table 2. Buck-boost converter modes

Mode	Switch state
s_1	$[s]_1 = 0, [s]_2 = 0$
s_2	$[s]_1 = 0, [s]_2 = 1$
s_3	$[s]_1 = 1, [s]_2 = 0$
s_4	$[s]_1 = 1, [s]_2 = 1$

For this particular case study assumed component values for the converter are given in Table 1. The matrices $\mathcal{A}_i$ and $\mathcal{B}_i$, $i \in \mathbb{Z}_{[0,2]}$ are defined as follows:

$$\mathcal{A}_0 = \begin{bmatrix} 0 & 0 \\ 0 & -\frac{R_L}{L} \end{bmatrix}, \quad \mathcal{A}_1 = \begin{bmatrix} 0 & 0 \\ 0 & \frac{1}{C} \end{bmatrix}, \quad \mathcal{A}_2 = \begin{bmatrix} 0 & 0 \\ -\frac{1}{L} & 0 \end{bmatrix},$$
$$\mathcal{B}_0 = \begin{bmatrix} 0 & -\frac{1}{C} \\ 0 & 0 \end{bmatrix}, \quad \mathcal{B}_1 = \begin{bmatrix} 0 & 0 \\ 0 & 0 \end{bmatrix}, \quad \mathcal{B}_2 = \begin{bmatrix} \frac{1}{L} & 0 \\ 0 & 0 \end{bmatrix}, \quad f = \begin{bmatrix} 0 \\ 0 \end{bmatrix}.$$

As each switch $[s]_i$ has two possible positions, the converter can function in four modes. Possible switch states and associated modes are given in Table 2. The construction of CT-SA model follows directly as shown in Section 3.1. Then this model is discretized, as shown in Section 3.2, with the sampling time $T_s = 10\mu$s to obtain the DT-B model.

To obtain the PWA approximation of DT-B model one has to define each region $\mathbb{P}_i$. The domain of variation of x, u and w,

$$\mathcal{D} := \mathbb{X} \times \mathbb{R}^2_{[0,1]} \times \mathbb{W},$$

where

$$\mathbb{X} := \{x \in \mathbb{R}^2 | -10 \leq [x]_1 \leq 20, -10 \leq [x]_2 \leq 10\},$$
$$\mathbb{W} := \{w \in \mathbb{R}^2 | 0 \leq [w]_1 \leq 20, 0 \leq [w]_2 \leq 1\}.$$

Note that only $[u]_2$ affects the $A(u)$. As such, the splitting of the space $\mathcal{D}$ is defined as follows,

$$\mathbb{P}_i := \mathbb{X} \times \mathbb{U}_i \times \mathbb{W}, \forall i \in \mathbb{Z}_{[1,4]},$$
$$\mathbb{U}_1 := \left\{u \in \mathbb{R}^2 | \quad 0 \leq [u]_2 < 0.25\right\},$$
$$\mathbb{U}_2 := \left\{u \in \mathbb{R}^2 | 0.25 \leq [u]_2 < 0.5\right\},$$
$$\mathbb{U}_3 := \left\{u \in \mathbb{R}^2 | \ 0.5 \leq [u]_2 < 0.75\right\},$$
$$\mathbb{U}_4 := \left\{u \in \mathbb{R}^2 | 0.75 \leq [u]_2 \leq 1\right\}.$$

Next, the procedure described in Section 3.3 yields the DT-PWA model for the system.

Totally six observers are compared in this case-study, i.e., single and multiple gain versions of observers for CT-SA, DT-PWA and DT-B system models. The partition $\mathcal{U} := \{\mathbb{U}_i\}$, $i \in \mathbb{Z}_{[1,4]}$ was employed in the observer synthesis for the DT-B model.

5.1 Simulation results

The first set of simulations is obtained as follows. The converter behaviour was simulated with the continuous-time switched affine model with initial conditions $x = \begin{bmatrix} 0 \\ 0 \end{bmatrix}$ and controlled by PWM signal as shown in Figure 2 with constant duty-cycle ratios $u = \begin{bmatrix} 0.5 \\ 0.37 \end{bmatrix}$. The sampling is performed twice each PWM period. The initial conditions of the observer are $\hat{x} = \begin{bmatrix} 2 \\ 3 \end{bmatrix}$.

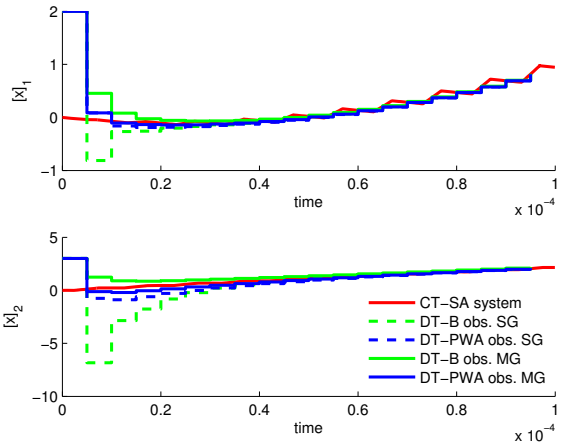

Fig. 4. Convergence of DT observers.

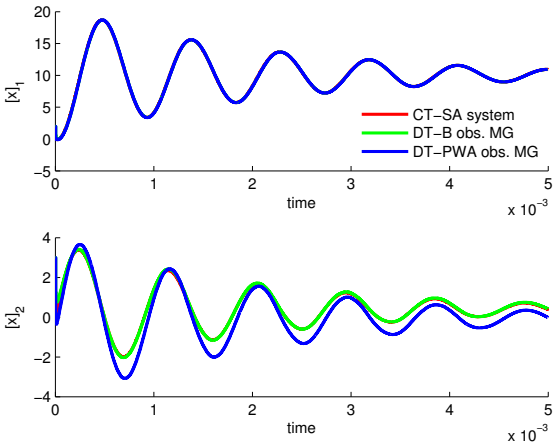

Fig. 5. Stationary error in the state estimation with DT-PWA observer.

Let begin by analysing the convergence of DT observers. Figure 4 shows the simulation results of DT-PWA and DT-B observers, both single gain (SG) and multiple gain (MG) versions, with measurements from the CT-SA model of the converter.

As expected, all observers converge successfully to the actual state values. Nevertheless, it is noticeable that single gain observers are considerably more aggressive comparing to multiple gain counterparts. This happens, regardless to the fact that the same $\rho = 0.9$ was used during synthesis. The explanation of this fact comes from that a single gain observer has to stabilize the error dynamics on larger domain, thus higher gain may be required.

DT-PWA observers show impressive convergence in Figure 4. However, one should remember that the DT-PWA model is only an approximation of the real converter dynamics, and its accuracy is expected to drop when the duty-cycle ratio is near the boundary of the a region $\mathbb{P}_i$. The same simulation is repeated for duty-cycle ratios of $u = \begin{bmatrix} 0.5 \\ 0.48 \end{bmatrix}$. The result of the simulation are reported in Figure 5. Notice the offset in the trajectories of DT-PWA observers. It is clearly visible on $[x]_2$, and appears due to the mismatch in between the DT-PWA approximation and the DT-B converter model.

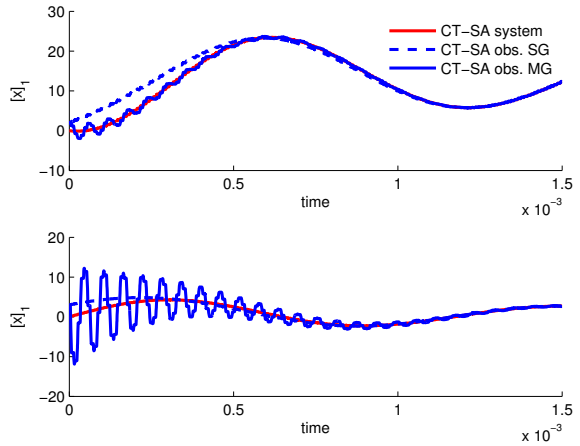

Fig. 6. Convergence of CT-SA observers.

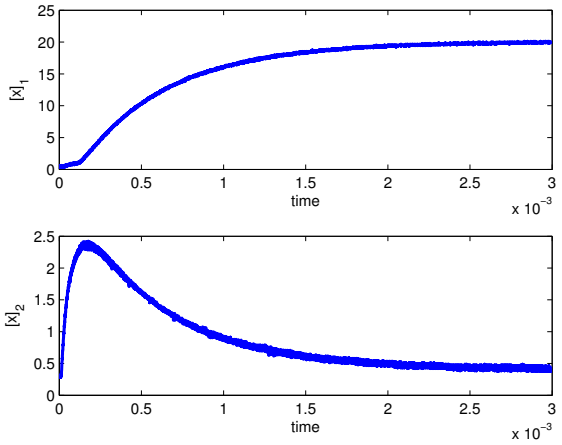

Fig. 7. Start-up of the buck-boost converter in closed-loop with an affine feedback from estimated states.(Oscilloscope measurements from real-life experimental platform.)

The CT-SA observers were simulated in the same environment as DT observers from Figure 4. The result is shown in Figure 6.

For this particular example, the convergence of the CT-SA observers is slower comparing to DT observers. Nevertheless, the value of such observer comes from the fact that it estimates the true switching trajectory of the states and not only the average value. This type of observers may be especially beneficial in case of converters which are controlled with variable frequency PWM signal.

5.2 Experimental results and final considerations

Typically, observers are used in combination with state feedback. To show the consistency of the results presented in this paper a start-up of the buck-boost converter in closed loop with the affine feedback from the estimated states with DT-B observer with single gain are shown in Figure 7. For more details on the used control law, interested reader is referred to [Spinu et al., 2011a]. The obtained result is consistent with the start-up of the converter when all states are measurable.

There are a few unanswered questions left in this paper, which constitute the object of future research. Probably the most important task would be to estimate the state of uncontrolled switches at each given moment of time. Another aspect is that the converter dynamics may not be fully observable for some modes, e.g., the inductor current is unobservable when $[s]_2 = 0$ or $[u]_2 = 0$. In the particular case of the buck-boost converter the gain associated to inductor current several orders of magnitude smaller for unobservable modes comparing to fully observable ones. Nevertheless, more in depth investigation of these phenomena is required.

6. CONCLUSIONS

In this paper a short review of observer design techniques tailored to needs of power-electronics community was given. Apart from existing solution to state estimation of continuous-time switched affine and discrete-time PWA systems, a new solution was designed for state estimation of systems with input-induced bilinearity. The convergence analysis and practical suitability to state estimation in power converters was demonstrated on the example of a buck-boost converter. Compelling simulation results coupled with successful experiments encourage further development observer synthesis methods and advanced observer-based control techniques for power converters.

REFERENCES

A. Alessandri and P. Coletta. Design of Luenberger observers for a class of hybrid linear systems. In *Proc. of Hybrid Systems: Computation and Control*, pages 7–18, Rome, 2001a.

A. Alessandri and P. Coletta. Switching observers for continuous-time and discrete-time linear systems. In *Proc. of the American Control Conference*, pages 2516–2521, 2001b.

S. Boyd, L. El Ghaoui, E. Feron, and V. Balakrishnan. *Linear Matrix Inequalities in System and Control Theory*. SIAM, 1994.

P. Cortés, M.P. Kazmierkowski, R.M. Kennel, D.E. Quevedo, and J. Rodríguez. Predictive control in power electronics and drives. *IEEE Transactions on industrial electronics*, 55(12): 4312–4324, dec. 2008.

W.P.M.H. Heemels, M. Lazar, N. van de Wouw, and A. Pavlov. Observer-based control of discrete-time piecewise affine systems: Exploiting continuity twice. In *2008 47th IEEE Conference on Decision and Control*, pages 4675–4680. IEEE, 2008.

A. Lj. Juloski, W. P. M. H. Heemels, Y. Boers, and F. Verschure. Two approaches to state estimation for a class of piecewise affine systems. In *Proc. of Conference on Decision and Control 2003*, Maui, Hawaii, USA, 2003.

M. K. Kazimierczuk. *Pulse-width modulated DC-DC power converters*. Wiley, 2008.

S. Mariéthoz, S. Almér, M. Bâja, A. G. Beccuti, D. Patino, A. Wernrud, J. Buisson, H. Cormerais, T. Geyer, H. Fujioka, U. T. Jönsson, C.-Y. Kao, M. Morari, G. Papafotiou, A. Rantzer, and P. Riedinger. Comparison of hybrid control techniques for buck and boost DC-DC converters. *IEEE Transactions on Control Systems Technology*, 18(5):1126 – 1145, sep. 2010. ISSN 1063-6536.

V. Spinu, M. Lazar, and G. Bitsoris. Constrained stabilization of a two-input buck-boost DC/DC converter using a set-theoretic method. In *American Control Conference*, pages 5394–5399, 29 2011-july 1 2011a.

V. Spinu, M Lazar, and P. P. J. van den Bosch. An explicit state-feedback solution to constrained stabilization of DC-DC power converters. In *IEEE Conference on Control Applications*, pages 1112–1118, september 2011b.